A Study on Bose-Einstein Condensation of Pions produced in Proton+Proton Collisions at the Large Hadron Collider using Non-Extensive Statistics

MSc THESIS

by

Anil Kumar Pradhan

DISCIPLINE OF PHYSICS

INDIAN INSTITUTE OF TECHNOLOGY INDORE

KHANDWA ROAD, SIMROL, INDORE-453552 INDIA

A Study on Bose-Einstein Condensation of Pions produced in Proton+Proton Collisions at the Large Hadron Collider using Non-Extensive Statistics

A THESIS

Submitted in partial fulfillment of the

requirements for the award of the degree

of

Master of Science

by

Anil Kumar Pradhan

(Roll No. **1803151004**)

Under the guidance of

Prof. Raghunath Sahoo

DISCIPLINE OF PHYSICS

INDIAN INSTITUTE OF TECHNOLOGY INDORE

JUNE 2020

INDIAN INSTITUTE OF TECHNOLOGY INDORE

CANDIDATE'S DECLARATION

I hereby certify that the work which is being presented in the thesis entitled "**A Study on Bose-Einstein Condensation of Pions produced in Proton+Proton Collisions at the Large Hadron Collider using Non-Extensive Statistics"** in the partial fulfillment of the requirements for the award of the degree of **MASTER OF SCIENCE** and submitted in the **DISCIPLINE OF PHYSICS, Indian Institute of Technology Indore**, is an authentic record of my own work carried out during the time period from July 2019 to June 2020 under the supervision of Prof. Raghunath Sahoo, Associate Professor, Indian Institute of Technology Indore.

The matter presented in this thesis has not been submitted by me for the award of any other degree of this or any other institute.

Anil Kumar Pradhan
16/06/2020

(Anil Kumar Pradhan)

This is to certify that the above statement made by the candidate is correct to the best of my knowledge.

M.Sc. Thesis Supervisor
(**Prof. Raghunath Sahoo**)

Anil Kumar Pradhan has successfully given his M.Sc. Oral Examination held on **:** 22.06.2020

M.Sc. Thesis Supervisor
Date: 07.07.2020

Convener, DPGC
Date:07.07.2020

PSPC Member 1
Date:07.07.2020
(Dr. M. Mahato)

PSPC Member 2
Date: 07.07. 2020
(Dr. Satyajit Chatterjee)

ACKNOWLEDGEMENTS

First and foremost I would like to express my deepest gratitude to my supervisor, Prof. Raghunath Sahoo for his valuable guidance and continuous encouragement. His simplicity and kindness, attention to detail, hard work, and patience have set an example for me. His incredible teaching manner and way of thinking inspired me a lot. I would also like to thank my PSPC committee members, Dr. Manavendra N. Mahato and Dr. Satyajit Chatterjee for their helps.

I would like to thank Dushmanta bhai for his wonderful support and wisdom. You supported me greatly and were always willing to help me in every situation regarding studies as well in life.

I would like to thank Golam bhai and Suman bhai for their great support and help always to clear concepts about any physics related questions. I would also like to thank my all lab mates for their continuous support.

Dedicated to My Family....

ABSTRACT

We have studied the pp collisions at the Large Hadron Collider (LHC) and estimated the requirements for the Bose-Einstein condensation in the pion gas formed in such collisions. We have used the Tsallis non-extensive statistics to estimate the transition temperature (T_c) required to form the condensation. We clearly observe that the T_c depends on the non-extensive parameter q. As q decreases the T_c increases and gradually approaches to the T_c obtained from the pion gas which is at equilibrium ($q = 1$). We also find a threshold of charged particle multiplicity below which the pion condensation is dominant.

Contents

List of Figures

Chapter 1

Introduction

1.1 What is High Energy Physics?

High Energy Physics (HEP) is the study of the most fundamental building blocks of the universe and their interactions at extreme energies. Everything in our universe that is visible to us consists of indivisible units which are known as the fundamental particles or elementary particles. The universe basically consists of two types of particles; fermions and bosons. Fermions have half integral spins and follow the Pauli's exclusion principle. The quarks, antiquarks, leptons and antileptons are of this category. Bosons, on the other hand, have integral spin, i.e. they don't follow Pauli's exclusion principle. All the gauge bosons such as the gluons, photons and W and Z bosons are from this category along with the mesons which are actually composite particles. The theory that describes all the elementary particles and their interactions, is called Standard Model (SM) of Particle Physics. A list of elementary particles is given in Fig.1.1.

These fundamental particles are controlled by four basic interactions or forces such as Strong force, Weak force, Electromagnetic force and Gravitational force. The SM of particle physics describes the relation between all the particles and the four fundamental forces. Just after the Big Bang Nucleosynthesis (BBN), nearly few millionths of a second, the universe was filled with an extremely hot, dense plasma consisting of all kinds of particles moving nearly with the speed of light. This hot mixture was mostly filled

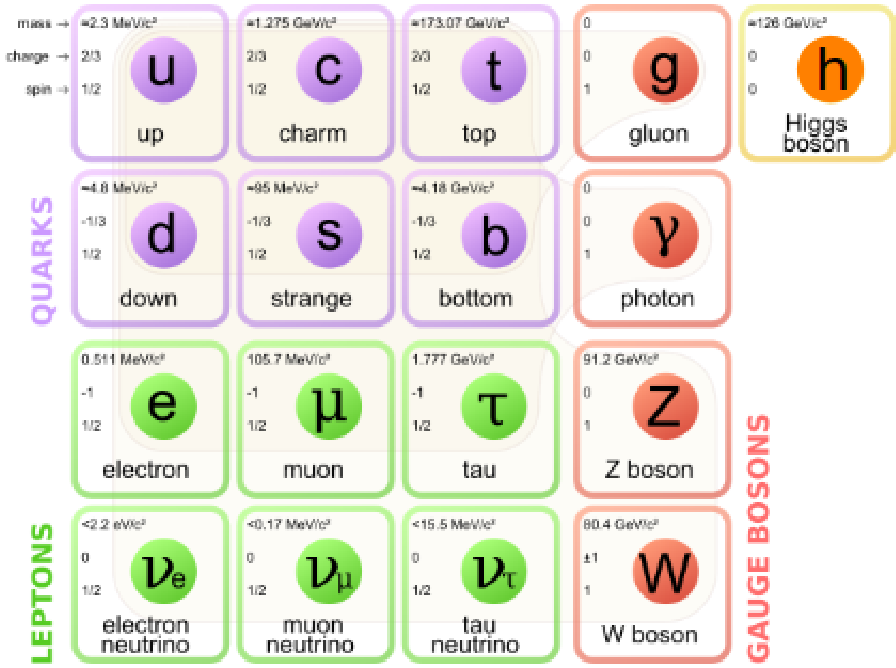

Figure 1.1: Standard model of elementary particles (source : online)

with quarks and gluons, which are the fundamental constituents of matter and know as Quark-Gluon Plasma (QGP). The QGP state is studied by a theory called Quantum Chromodynamics (QCD), which is the theory of strong interaction. Gluons are the force carriers for the strong force which help to bind the quarks together. The QCD predicts that quarks and gluons can exist in a deconfined state (QGP) in which they can move to distances even large than the typical hadron size. Hadrons or ions with high energies are made to collide under suitable experimental conditions to probe the dense nuclear matter similar to which was present in the evolutionary phase of the early universe. In the high energy heavy ion collisions, there is a possibility of formation of the QGP at extreme conditions of temperature and energy density.

In particle physics, elementary particles means the particles which have no substructure or point-like objects that are constituents of matter. Therefore, we depend on the spatial resolution of the probe used to investigate the possible structure/sub-structure. Say, two points of an object can just be resolved as separate by a distance Δr apart. Assuming that the probing beams themselves consist of point-like particles like electrons or positrons, this resolution is limited by the de Broglie wavelength of these beam particles, which is given by $\lambda = h/p$, where p is the momentum of the beam particle and h is the Planck's constant. Hence beams of high momentum have short de Broglie wavelengths and thus have high resolution [1].

1.2 Heavy-Ion Collisions

The general consensus among the scientific community is that our universe was created through Big Bang. Immediately after the Big Bang, the fundamental particles were produced, followed by a phase where the universe was filled with a state of matter know as QGP. The initial conditions after the Big Bang could be studied by achieving such high temperatures and/or densities in the laboratories. One of the ways to study the properties of nuclear matter in the laboratory is through high energy heavy-ion collisions. These collisions provide the unique possibility to create and investigate the nuclear matter at high temperatures and high densities in the laboratory. Collision of two nuclei at relativistic energies gives us information about particle production mechanism. Powerful accelerators collide heavy-ions or hadrons at an energy of the order of some trillion electronvolts (TeV). When two Lorentz contracted nuclei collide at very high energies, the region where they overlap is very thin in the longitudinal direction, much like an almond shape. This energetic interaction results in the formation of a possible state of the QGP. The QGP exists at very high temperature and/or energy density and consists of asymptotically free quarks and gluons, otherwise known as partons. The created fireball then expands and cools down gradually until the produced particles reach kinetic freeze-out.

The first heavy-ion collisions experiment was performed in the 1970s and 80s with fixed target nuclei at the Alternating Gradient Synchrotron (AGS) in the Brookhaven and the Super Proton Synchrotron (SPS) in the European Laboratory for Nuclear Research (CERN) with the center of mass energies of 33 GeV and 400 GeV respectively. Most of the recent experiments are performed at the Relativistic Heavy Ion Collider (RHIC) in the Brookhaven and the A Large Ion Collider Experiment (ALICE) detector at the Large Hadron Collider (LHC) at the CERN, where the energy has reached upto 13 TeV.

1.2.1 Kinematic Variables

In high energy physics, all the particles are treated as relativistic due to their speed being nearly close to the speed of light. According to Einstein's special theory of relativity, the velocity of light (c) always remains constant in any inertial frame of reference. All the physical observables like position, momentum are treated as four components of coordinate vectors. For relativistic heavy-ion collision, it is more convenient to use the kinematic variables as they have simple forms under Lorentz transformation with the change of reference frame. In Fig.1.2, the Z-axis is the beam axis of the

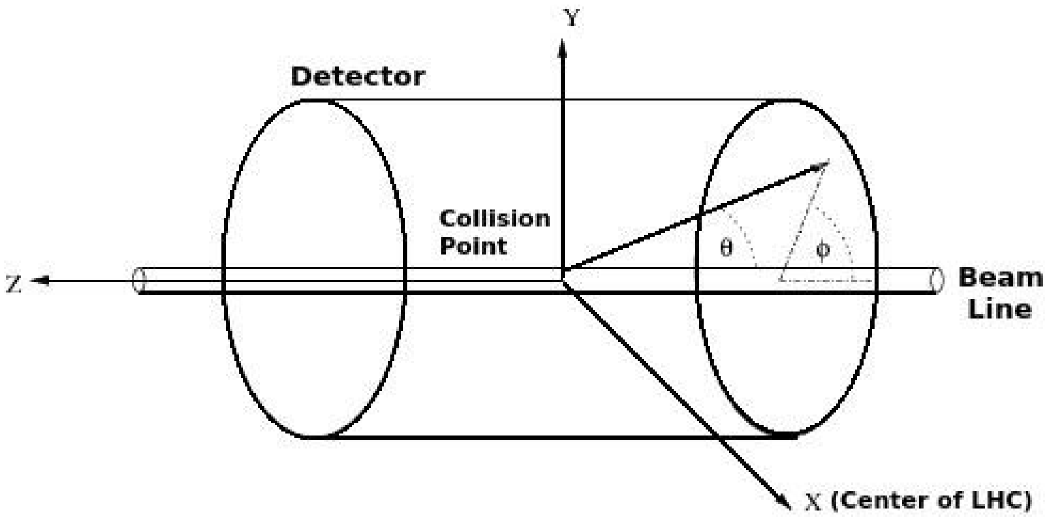

Figure 1.2: Coordinates of particle collision. (Source : online)

collision plane, the XY plane is treated as the transverse plane. The angle between the produced particle and the Z-axis is denoted by θ which is called as the polar angle. Azimuthal angle ϕ is the angle measured from the X-axis in the transverse plane. There are some other kinematic variables as discussed below.

Rapidity

As the velocities are not additive i.e. non-linear in successive transformation, a new kinematic variable was introduced called rapidity [1]. It changes by an additive constant under successive Lorentz boost. Rapidity is a dimensionless quantity and is given by,

$$y = \frac{1}{2} \ln \left(\frac{E + p_z}{E - p_z} \right), \tag{1.1}$$

where E and p_z are the energy and longitudinal momentum component of the particle respectively.

Pseudorapidity

For highly relativistic particles, the z component of the momentum is too large. Therefore, it is too difficult to get total momentum vector at higher values of rapidity. To overcome this limitation a quantity almost similar to rapidity called pseudorapidity (η) is defined and which is given by,

$$\eta = - \ln \left(tan \frac{\theta}{2} \right). \tag{1.2}$$

Pseudorapidity is particularly useful in hadron colliders such as the LHC, where the composite nature of the colliding protons is such that interactions rarely have their center of mass frame coincide with the detector rest frame. In addition, a knowledge of energy and momenta of the particles is not necessary, like it is for rapidity variable. For rapidity, particle identification is required, which is a very difficult task in high energy experiments, particularly at higher momenta. Just knowing the position of the hit points on the detector, contrary helps us to have information about psedurapidity.

1.3 Quark-Gluon Plasma (QGP)

The QGP is predicted by the theory of strong interaction i.e. Quantum Chromodynamics (QCD). The QGP occurs at extremely high temperatures and/or high baryon densities. This state consists of asymptotically free strongly interacting partons (quarks and gluons) and is an analogy to electromagnetic plasma. This state of matter has been produced at the laboratories such as the RHIC and the LHC.

The QGP is a thermally equilibrated system where the partons are deconfined from the hadrons so that the color degrees of freedom become explicit in nuclear rather than the nucleonic volume [2]. This can be achieved either by heating the nuclei to ultra-high temperatures i.e. hundreds of MeVs (1 MeV $= 1.16 \times 10^{10}$ Kelvin), which is done at the RHIC and the LHC energies or by compression of nuclei so as to diffuse the hadronic boundaries, which may be happening in the cores of neutron stars.

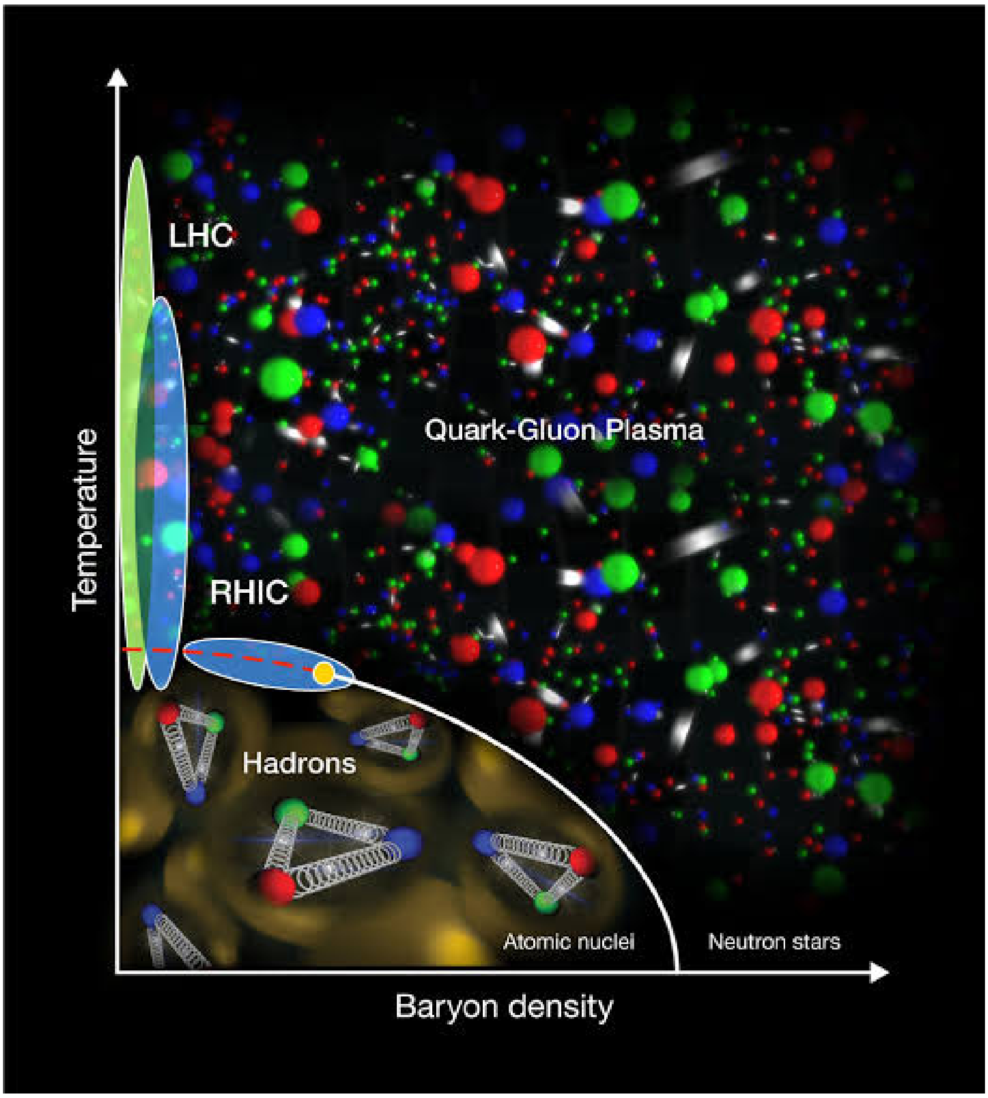

Figure 1.3: A schematic of the QCD phase diagram. Source: [3].

In Fig.1.3, the temperature is plotted as a function of the baryon density of the system. The phase diagram has two scenarios, one is a high temperature and low baryon density which corresponds to an early universe that might have existed billions of years ago and the other is the low temperature and high baryon density which corresponds to different astrophysical objects like neutron stars.

The deconfined phase of quarks and gluons is separated by a first order phase transition from the confined hadronic matter, which ends with a possible critical end-point (CP) [3]. So we observe a cross-over transition in the RHIC and LHC energy regimes. The exploration of this QCD phase diagram and the search for the CP has been a frontier of high energy nuclear research for decades. The critical energy density and temperature required for such deconfinement transition is $\varepsilon_c = 1$ GeV/fm^3 and $T_c \approx 150 - 170$ MeV [4].

1.3.1 The Space-Time Evolution

The Fig.1.4 shows that the space-time evolution in hadronic and heavy-ion collisions are complex phenomena involving various degrees of freedom at different space-time coordinates. After the collisions of heavy-ions, the system goes through a pre-equilibrium phase, which is followed by a deconfined QGP phase. After that a possible mixed phase occurs which should show the first order phase transition signatures. Then, hadronization occurs, forming composite hadrons from the primordial partonic matter. There is a possible phase transition from the QGP to hadron gas, this point is marked by the critical temperature (T_c). After that the chemical composition of the system is frozen in which inelastic collisions begin to cease, making the particle ratios fixed with time. This point is treated as chemical freeze-out boundary for the particles. This is characterized by the chemical freeze-out temperature (T_{ch}) and the baryochemical potential (μ_B) of the system. At this point a statistical hadron gas model works, which ignores the interactions treating the system as an ideal gas. Now, the final state particles then fly toward the detectors and the mean free path of the system becomes higher than the system size, making the particles col-

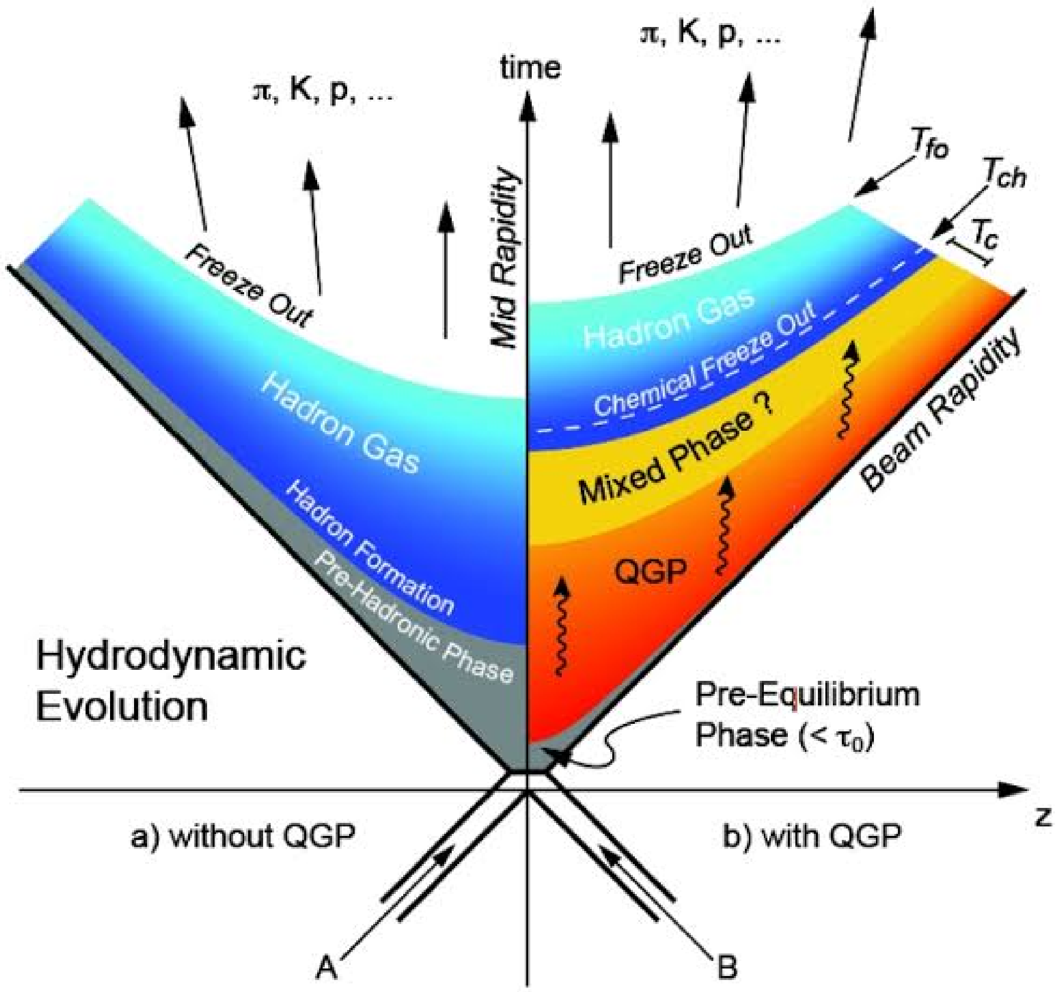

Figure 1.4: A schematic diagram space-time evolution in hadronic collisions, compared with heavy-ion collisions. Source: [3]

lide infrequently with each other. At this point, the transverse momentum distribution of the system is fixed with time in which the elastic collisions stop. This is called kinetic freeze-out and after that the particles are finally detected at the detectors.

The left part of the Fig.1.4 describes the space-time evolution of a collision without the QGP formation. Generally low multiplicity *pp* collisions fall under this category. After the collision, the system goes through a pre-hadronic phase and then the chemical freeze-out occurs without the QGP phase. Then the produced hadrons attain kinetic freeze-out and finally are detected at the detectors.

1.4 Motivation

The particles which have an integral spin, are called bosons and obey the Bose-Einstein condensation. Pions are spin-0 bosons with three isospin states, namely π^+, π^0, π^-. These are the lightest mesons (hadrons are subdivided to baryon and meson). Baryon has odd half integer spin and meson has integer spin and are produced abundantly in any ultra-relativistic heavy-ion collisions, with yield almost 80 percent of the total number of particles produced (mostly pions, less percent of kaons, protons and other particles). This is the reason we have considered pion gas system to study for our purpose.

When two Lorentz contracted nuclei collide at ultra-relativistic energies, the produced fireball contains partons (quarks and gluons) as the degrees of freedom. The hot and dense fireball then gradually expands and cools down. The hadrons start forming within the system and finally the particle production stops when the temperature goes down to the kinetic freeze-out temperature. It is seen that at the LHC energies, the p_T-spectra of identified charged particles doesn't follow a thermalized Boltzmann-Gibbs statistics, which should be a high-temperature approximation of Fermi-Dirac and Bose-Einstein statistics, depending on if the particle is a fermion or boson, respectively. As a result, if we apply the Bose-Einstein (BE) distribution to study pion condensation in pp collisions, we may not get the accurate description of the system. This drives us toward using a non-extensive statistics.

In this work, we have considered a thermodynamically consistent version of non-extensive Tsallis statistics. Tsallis statistics is a generalization of previously known Boltzmann-Gibbs (BG), Fermi-Dirac (FD) and BE statistics, where a deformation parameter q is present. This parameter corresponds to the degree of deviation of the system from equilibrium to non-equilibrium condition. For the value $q = 1$, the whole statistics becomes the normal BG statistics at equilibrium condition. The non-extensive parameter, q, encodes the dynamics of the system, like degree of correlation, fluctuation etc.

Chapter 2

Statistical Mechanics

Statistical Mechanics is a branch of physics which considers how the overall behavior of a system of many particles is related to the properties of the particles themselves, or it establishes the interpretation of the macroscopic behavior of a system in terms of its microscopic properties. As its name implies, statistical mechanics is not concerned with the actual motion of individual particle of the system; but investigates instead what is most likely to happen. It is able to tell us, for instance, the probability that any particle has a certain amount of energy at a certain moment.

The methods of statistical mechanics are applied to draw inferences and making the conclusions of some average or most probable properties of large assemblies of electrons, atoms, molecules, quanta etc. Some scientists applied the statistical methods making the use of classical physics, and developed a sub-branch known as classical statistics or Maxwell-Boltzmann (MB) statistics. The MB statistics successfully explains many observable physical phenomenon like temperature, pressure, energy, entropy etc.; but it could not explain accurately several other experimentally observed phenomenon such as black-body radiation, specific heat at low temperature etc. To explain such phenomenon, scientists developed a new approach called quantum statistics. The quantum statistics is subdivided into two categories:

1. Bose-Einstein statistics
2. Fermi-Dirac statistics

2.1 Maxwell-Boltzmann Statistics

Classical particles such as gas molecules obey the MB statistics. The particles are identical and can be distinguishable. In quantum terms, the wave functions of such particles overlap to a negligible extent.

The MB distribution function states that the average number of particles $f_{MB}(E)$ in a state of energy E in a system of particles at absolute temperature T is,

$$f_{MB}(E) = \frac{g_i}{\exp(\frac{E-\mu}{kT})}, \tag{2.1}$$

where g_i is the degeneracy, μ is the chemical potential, k is the Boltzmann constant.

2.2 Quantum Statistics

The quantum statistics deals with all the quantum systems. Bosons and fermions obey quantum statistics and follow different statistical distributions.

2.2.1 Fermi-Dirac Statistics

The Fermi-Dirac (FD) statistics is obeyed by the particles that have odd-half integral spins ($\frac{1}{2}, \frac{3}{2}, \frac{5}{2}$....), and are called fermions. Fermions are identical quantum particles and can not be distinguishable. Fermions obey Pauli's exclusion principle, which means the maximum number of particles (with spin s) that can occupy the same state is $(2s + 1)$. The wave function of a system of fermions changes upon the exchange of any pair of the particles.. The wave function of this kind is called antisymmetric. Only one fermion can occupy in a particular quantum state of the system.

Let us consider a system of two particles, 1 and 2, one of which is in state a and other in state b. When the particles are distinguishable, there are two possibilities for occupancy of the states, given as below

$$\psi_I = \psi_a(1)\psi_b(2), \tag{2.2}$$

$$\psi_{II} = \psi_a(2)\psi_b(1). \tag{2.3}$$

When the particles are not distinguishable, we can tell which of them is in which state. If they are fermions. the system is described by antisymmetric wave function. So the Eq.(2.2) and Eq.(2.3) can be written as,

$$\psi_F = \frac{1}{\sqrt{2}}[\psi_a(1)\psi_b(2) - \psi_a(2)\psi_b(1)], \tag{2.4}$$

where $\frac{1}{\sqrt{2}}$ is the normalization factor.
The distribution function for fermions is given by,

$$f_{FD}(E) = \frac{g_i}{\exp\left(\frac{E-\mu}{kT}\right) + 1}. \tag{2.5}$$

2.2.2 Bose-Einstein Statistics

The Bose-Einstein statistics is obeyed by the particles that have zero or integral spins, which are called bosons. Bosons are identical and indistinguishable. Bosons do not obey the exclusion principle, and the wave function of a system of bosons is not affected by the exchange of any pair of them. A wave function of this kind is called symmetric, means any number of bosons can exist in the same quantum state of the system.

Similarly as the above section, when the particles are not distinguishable, we can not tell which of them is in which state. If they are bosons, by using Eq.(2.2) and Eq.(2.3), the symmetric wave function for the system is given by,

$$\psi_B = \frac{1}{\sqrt{2}}[\psi_a(1)\psi_b(2) + \psi_a(2)\psi_b(1)]. \tag{2.6}$$

The distribution for bosons can be written as,

$$f_{BE}(E) = \frac{g_i}{\exp\left(\frac{E-\mu}{kT}\right) - 1}. \tag{2.7}$$

2.2.3 Bose-Einstein Condensation

Statistical mechanics plays a very significant role in understanding the underlying behaviors of nature. From the study of system of gases to the white-dwarf stars, it has changed our perception of the physical world in numerous ways. One of the most astounding revelations of the statistical mechanics was the discovery of a new state of matter, called Bose-Einstein condensate, rightfully named after the two giants of twentieth century physics, Satyendra Nath Bose and Albert Einstein.

In 1924 Indian physicist Satyendra Nath Bose sent a paper to Albert Einstein in which he had derived the Planck's law for black-body radiation by treating the photons as particles of an ideal gas. Later Einstein predicted that at sufficiently low temperature the particles would condense into the lowest possible energy state of the system. This phenomenon is called Bose-Einstein Condensation (BEC). BEC is applicable to bosons which follow the Bose-Einstein (BE) statistics. The BE statistics describes one of the two possible ways in which a collection of non-interacting, indistinguishable particles may occupy a set of available discrete energy states at thermal equilibrium. BEC is called the fifth state of matter which is usually formed when a gas of bosons at low densities are cooled to a temperature very close to absolute zero. Under such conditions, a large fraction of the particles occupy the lowest possible energy state or zero momentum state, at which point the wave functions of the such particles interfere with each other and the effect is observed microscopically. This is possible because the bosons have integral spins and symmetric wave functions. All the bosons in a system below a particular low temperature (T_c), behave differently than fermions which obey Pauli's exclusion principle. For BEC, the distribution function is like as Eq.(2.7) (where $g_i = 1$),

$$f(E) = \frac{1}{\exp\left(\frac{E-\mu}{kT}\right) - 1}. \tag{2.8}$$

For our study on BEC in pion gas, we use a thermodynamically consistent non-extensive statistics. There is a non-extensive parameter in the system, which tells us that how much the system deviates from the equilibrium state. In proton-proton collisions, we consider the produced system to be away from thermodynamic equilibrium, as is evident from the p_T-spectra of identified particles. Hence to describe such a system, the right statistics would be Tsallis non-extensive statistics.

Chapter 3

Non-Extensive Statistical Mechanics

According to thermodynamics, entropy of a system is defined as a measurement of disorder of molecular motion of that system. Means, greater is the disorder of molecular motion of the system, greater is the entropy.

In statistical mechanics, the entropy is an extensive property of the thermodynamic system and its function is represented as probability distribution. It is a delicate and powerful concept to be carefully constructed for classes of systems. These systems share the same functional connection between the entropy and the set of probabilities of their microscopic states. The most known of such class is that which we shall refer to as the Boltzmann-Gibbs (BG). The BG entropy for a set of W discrete states is given by,

$$S_{BG} = -k \sum_{i=1}^{W} p_i \ln p_i \tag{3.1}$$

with

$$\sum_{i=1}^{W} p_i = 1, \tag{3.2}$$

where k is a positive constant called Boltzmann constant.
For a particular case of equal probabilities i.e. $p_i = \frac{1}{W}$, Eq.(3.1) becomes,

$$S_{BG} = k \ln W. \tag{3.3}$$

The Eq.(3.3) is a famous expression, as well as Eq.(3.1), and has been used in a variety of creative manners by scientists. If we compose two probabilistically independent subsystems say, A and B (with numbers of states respectively denoted by W_A and W_B), i.e., the joint probabilities factorize, $p_{ij}^{A+B} = p_i^A p_j^B (\forall (i,j))$, the entropy S_{BG} becomes additive [5]. i.e.

$$S_{BG}(A+B) = S_{BG}(A) + S_{BG}(B). \tag{3.4}$$

The extensive property of entropy is expressed as an additive quantity.

3.1 Non-extensive Statistics

The non-extensive statistical mechanics is the generalization of well known BG theory.

3.1.1 Mathematical Tools

Let us present here a possible metaphor for generalizing the BG entropy.

The simplest ordinary differential equation can be considered to be [6],

$$\frac{dy}{dx} = 0, (y(0) = 1) \tag{3.5}$$

so its solution is given by,

$$y = 1. \tag{3.6}$$

Now the second simplest differential equation we may consider

$$\frac{dy}{dx} = 1, (y(0) = 1) \tag{3.7}$$

and its solution is given by,

$$y = 1 + x, \tag{3.8}$$

whose inverse function is written as,

$$y = x - 1. \tag{3.9}$$

In similar manner, we may consider the following one,

$$\frac{dy}{dx} = y, (y(0) = 1) \tag{3.10}$$

whose solution is given by,

$$y = \exp(x). \tag{3.11}$$

And its inverse function is written as,

$$y = \ln x. \tag{3.12}$$

A property of logarithmic function is

$$\ln(x_A x_B) = \ln x_A + \ln x_B. \tag{3.13}$$

Now, let us consider,

$$\frac{dy}{dx} = y^q, (y(0) = 1; q \in R) \tag{3.14}$$

its solution is,

$$y = [1 + (1-q)x]^{\frac{1}{1-q}} \equiv \exp_q(x), (\exp_1(x) = \exp(x)). \tag{3.15}$$

Its inverse is written as,

$$y = \frac{x^{1-q} - 1}{1-q} \equiv \ln_q(x), (x > 0; \ln_1(x) = \ln(x)). \tag{3.16}$$

The Eq.(3.13) satisfies the property as the solution of Eq.(3.16)

$$\ln_q(x_A x_B) = \ln_q x_A + \ln_q x_B + (1-q)(\ln_q x_A)(\ln_q x_B). \tag{3.17}$$

Through the metaphor presented above, we may postulate the following generalization of Eq.(3.3):

$$S_q = k \ln_q W, (S_1 = S_{BG}, q = 1), \tag{3.18}$$

comparing with Eq.(3.17), entropy should be a non-additive quantity. similar to Eq.(3.1) the entropy can be written as,

$$S_q = k\langle \ln_q(1/p_i)\rangle. \tag{3.19}$$

Now, using Eq.(3.16) yields,

$$S_q = k\frac{1 - \sum_{i=1}^{W} p_i^q}{q-1}. \tag{3.20}$$

The non-additive entropy is written as,

$$S_q(x_A x_B) = S_q x_A + S_q x_B + (1-q)(S_q x_A)(S_q x_B). \tag{3.21}$$

This q parameter is generally known as non-extensive parameter or deformation parameter, which describes the non-extensive properties of any system.

There is a probability distribution derived from the maximization of the Tsallis entropy, i.e., Eq.(3.18) under appropriate constraints called Tsallis distribution.

3.2 Tsallis Distribution

Tsallis distribution function is the generalized form of the BG distribution function.

The Tsallis form of the Fermi-Dirac (FD) distribution as Eq.(2.5) is given by (putting $g_i = 1$ and $k = 1$ in natural unit),

$$f_q^{FD}(E) = \frac{1}{\exp_q(\frac{E-\mu}{T}) + 1}. \tag{3.22}$$

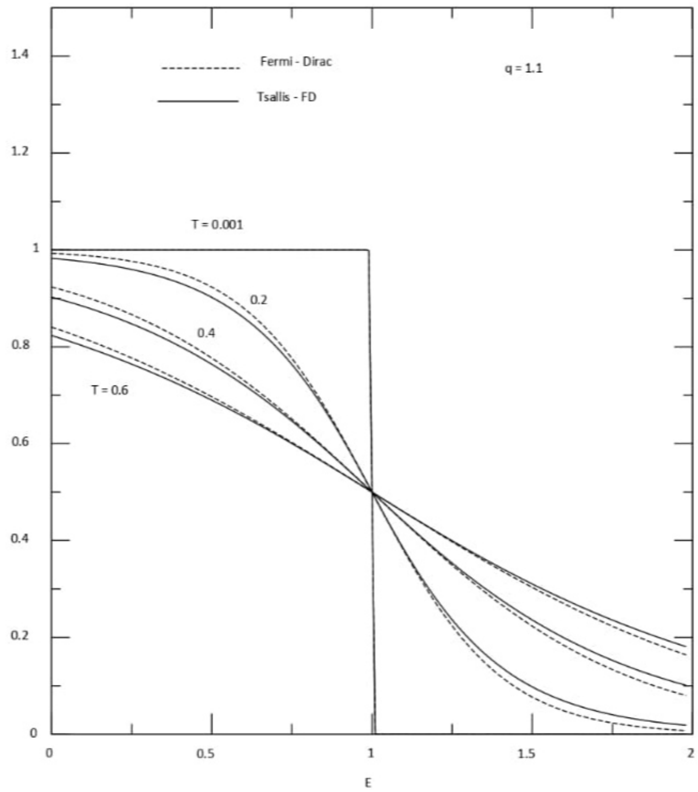

Figure 3.1: Comparison between the FD and the Tsallis-FD distribution as a function of the energy E, keeping the Tsallis parameter q fixed, for various values of the temperature T. The chemical potential (μ) is kept equal to 1 in all curves, and the units are arbitrary [9].

The Fig.3.1 shows that the numerical difference between the Eq.(2.5) and the Eq.(3.22) is small, for a value of $q = 1.1$.

The high energy heavy-ion collisions provide opportunity to study the nuclear matter under extreme conditions, i.e. at high temperature and/or density. So there is a possibility of a large number of particle production in the final state of A+A and pp collisions. The statistical models are suitable to describe this particle production mechanism. Such a statistical description of transverse momentum (p_T) of the final state particle production in high energy collisions has been proposed to follow a thermalized Boltzmann type of distribution as given by [7],

$$E\frac{d^3\sigma}{d^3p} \approx C \exp\left(-\frac{p_T}{T}\right). \tag{3.23}$$

To take into account for high p_T and low p_T region of the spectra, a power-law in p_T has been proposed, which empirically accounts for the possible QCD contributions [8], i.e.

$$E\frac{d^3\sigma}{d^3p} = C\left(1 + \frac{p_T}{p_0}\right)^{-n}, \tag{3.24}$$

for $p_T \longrightarrow 0, \exp(-\frac{np_T}{p_0})$

and for $p_T \longrightarrow \infty, (\frac{p_T}{p_0})^{-n}$

where T is the effective temperature i.e. $T = \frac{p_0}{n}$.

A thermodynamically consistent non-extensive distribution function is given by [9],

$$F(m_T) = C_q\left[1 + (q-1)\frac{m_T}{T}\right]^{-\frac{1}{q-1}}, \tag{3.25}$$

where m_T is the transverse mass, q is the non-extensive parameter which measures the degree of deviation from equilibrium.

The above expression is thermodynamically consistent, i.e. the first and second laws of thermodynamics lead to two differential relations must be satisfied [9, 10]:

$$d\epsilon = Tds + \mu dn, \tag{3.26}$$

$$dP = sdT + nd\mu, \tag{3.27}$$

where $\epsilon = U/V$, $s = S/V$ and $n = N/V$ are the energy, entropy and particle densities respectively, and P, μ, T, U, S, V and N are the pressure, chemical potential, temperature, internal energy, entropy, volume and number of particles respectively. The Maxwell relations given below follow from this:

$$T = \left.\frac{\partial\epsilon}{\partial s}\right|_n, \tag{3.28}$$

$$\mu = \left.\frac{\partial\epsilon}{\partial n}\right|_s, \tag{3.29}$$

$$n = \left.\frac{\partial P}{\partial \mu}\right|_{T}, \tag{3.30}$$

$$s = \left.\frac{\partial P}{\partial T}\right|_{\mu}. \tag{3.31}$$

The following thermodynamics relation must also be satisfied:

$$\epsilon + P = Ts + \mu n. \tag{3.32}$$

The proof of thermodynamical consistency of the parameter T in Eq.(3.25) is satisfied by [9],

$$T = \left.\frac{\partial U}{\partial S}\right|_{N,V}, \tag{3.33}$$

hence the parameter T of a system obeying Tsallis distribution.

Chapter 4

Bose-Einstein Condensation and Non-extensivity

We have taken advantage of the usefulness of a thermodynamically consistent Tsallis distribution function to explore the possibility and study pion condensation in the system produced in high energy pp collisions.

The Tsallis statistics of q-generalized framework has already been used to study BEC in liquid Helium (He_2^4) [11]. Whenever a system is subjected to temperature fluctuation, the non-equilibrium generalized statistical mechanics plays a crucial role. With zero spin, a He_2^4 is a boson and obeys BE statistics, and thus exhibits BEC at low temperature. Similarly, as pions fall under the group of bosons, it would be interesting to see whether the pion gas formed after a high energy pp collision shows any sign of BEC at such high temperatures.

4.1 Bose-Einstein Condensation of Pions

In ultra-relativistic high energy collisions, large amount of pions are produced. The temperature reached in the high energy collisions are of MeV scale which is about 10^{10} K [14]. This temperature is astronomically higher than the temperature required for BEC for cold atoms such as He_2^4 [11]. The pion system would have much smaller volume with high density and different interactions are involved in the formation of high temperature BEC. Thus the properties of a BEC for pions would be different from the low temperature BEC. An observation of the BEC signal of pions is dominant for pp collisions at $\sqrt{s} = 70$ GeV [12].

The aim of relativistic heavy-ion collisions is to understand the phases of Quantum Chromodynamics (QCD) matter. Especially, these collisions give us an opportunity to characterize the Quark-Gluon Plasma (QGP) phase and subsequent hadronic phase. To study the information about these phases, some models are used such as thermal models and hydrodynamic models. Thermal models mainly assume thermodynamic equilibrium to explain the hadronic yields. Whereas hydrodynamic models which use local thermodynamic equilibrium, are not quite good to explain the high momentum part of the pion p_T-spectra.

To explain these, the chemical non-equilibrium in the formation of the hadronic matter is assumed by Viktor Begun et.al [13, 14]. They have studied in the heavy-ion collisions that the chemical non-equilibrium brings up the non-zero value of chemical potential (μ) which is closer to the critical value of μ needed for BEC of pions. However, any contribution of non-equilibrium can exist in small systems like that formed in *pp* collisions, although in the LHC *pp* collisions the baryon chemical potential (μ_B) is taken as zero. Further, the system formed in *pp* collisions can be taken as reference to interpret the results of heavy-ion collisions. So it is of great significance to understand the formation of BEC like features in small systems formed in *pp* collisions. Thus we investigate the possibility of BEC in pion gas formed in *pp* collisions and compare the results with the heavy-ion collisions, to find the link between the two systems.

At the RHIC and the LHC energies, it is observed that the p_T-spectra of *pp* collision systems deviate from the standard thermalized BG distribution. In such cases, the Tsaliis distribution describes the p_T-spectra very well. The non-extensive parameter q gives the degree of deviation from equilibrium, for $q = 1$ suggests the equilibrium condition (BG scenario).

4.2 Mathematical Formulation

The Bose-Einstein (BE) distribution given by Eq.(2.8) (putting $k = 1$ in natural unit)

$$f(E) = \frac{1}{\exp(\frac{E-\mu}{T}) - 1}. \tag{4.1}$$

By using the above formula, we calculate the particle multiplicities as [13]

$$\mathrm{N} = \int_0^\infty \frac{d^3x d^3p}{h^3} \frac{g}{\exp\left(\frac{\sqrt{p^2+m^2}-\mu}{T}\right)-1}$$

$$\simeq V \int_0^\infty \frac{d^3p}{(2\pi)^3} \frac{g}{\exp\left(\frac{\sqrt{p^2+m^2}-\mu}{T}\right)-1}, \tag{4.2}$$

where g is the degeneracy of the particle, p is the momentum, m is the mass of the particle, T is the temperature of the system and μ is the chemical potential.

For our consideration of pion gas, $g = 2$ and $m \to m_\pi$. The integral over the space co-ordinates gives us the volume of the system V. In the thermodynamic limit, $V \to \infty$, we can write Eq.(4.2) as separate terms for $p = 0$ and $p > 0$, [13]

$$N \simeq \frac{1}{\exp(\frac{m_\pi-\mu}{T})-1} + V \int_0^\infty \frac{d^3p}{(2\pi)^3} \frac{1}{\exp\left(\frac{\sqrt{p^2+m_\pi^2}-\mu}{T}\right)-1}$$

$$\Rightarrow N_{\text{total}} = N_{\text{condensation}} + N_{\text{excited}}. \tag{4.3}$$

By taking Tsallis non-extensivity into account, the BE distribution function changes to,

$$f(E) = \frac{1}{\left[\exp_q(\frac{E-\mu}{T})-1\right]^q}. \tag{4.4}$$

Here, the non-extensive exponential function is defined as in Eq.(3.15) [9],

$$\exp_q(x) = [1+(q-1)x]^{1/q-1}, (x > 0). \tag{4.5}$$

The Eq.(4.3) is defined as the total number of particles in which the first term is the number of particles in the condensate and second term is the number of particles in the excited state, and it becomes,

$$N \simeq \frac{1}{\left[\exp_q(\frac{m_\pi - \mu}{T}) - 1\right]^q} + V \int_0^\infty \frac{d^3p}{(2\pi)^3} \frac{1}{\left[\exp_q\left(\frac{\sqrt{p^2+m_\pi^2}-\mu}{T}\right) - 1\right]^q}. \tag{4.6}$$

The formula for the critical temperature is given by [12],

$$T_c = 1.4 \times \rho^{1/3}, \tag{4.7}$$

where ρ is the number density of the system which is given by the formula,

$$\rho = g \int \frac{d^3p}{(2\pi)^3} \left[1 + (q-1)\frac{E-\mu}{T}\right]^{\frac{-q}{q-1}}. \tag{4.8}$$

4.3 Results and Discussion

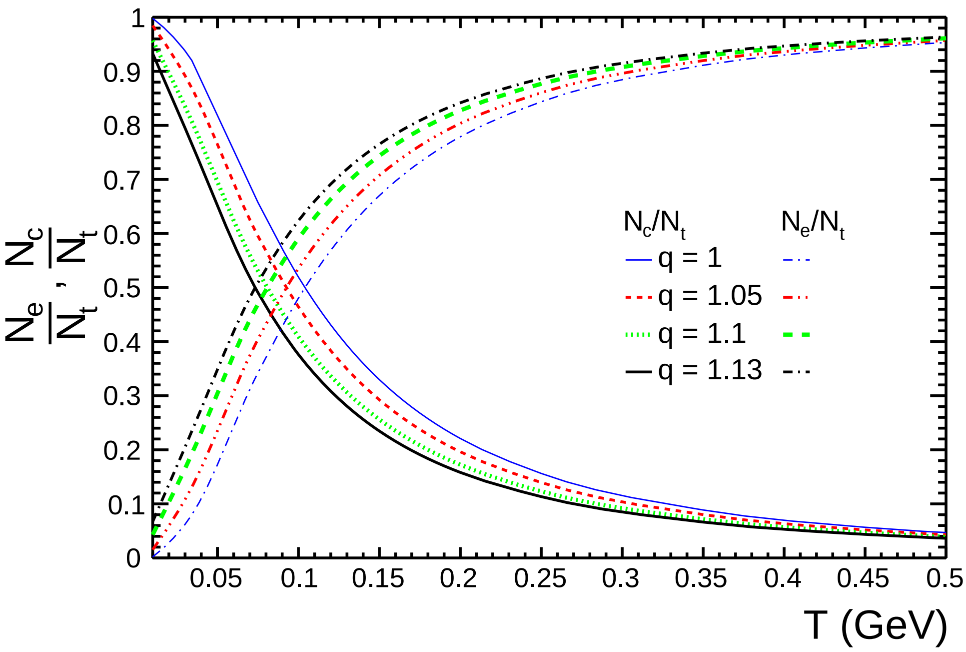

Figure 4.1: (Color online) Ratios of number of particles in the condensate with total number of particles and the number of particles in the excited state with total number of particles as a function of temperature for pion gas.

In Fig.4.1, we have plotted the ratios of $N_{\text{condensation}}/N_{\text{total}}$ and $N_{\text{excited}}/N_{\text{total}}$ as a function of temperature by using Eq.(4.6). We have taken some random values of temperature and estimated the ratios at particular q values. Here we have assumed a constant value of the volume of the system with the system radius of 1.2 fm. This volume roughly denotes the chemical freeze-out volume of the fireball formed in pp collisions. As calculating the kinetic freeze-out volume of a system is not trivial, we have used this approximation. This would have a great impact on the outcome, as higher volume would mean lower density and thus the possibility of BEC would vary. But as a safe guess, we have started with this approximation. We clearly see that the crossing points of the ratios which are the transition temperatures (T_c) are q dependent. This is an interesting finding, since we know that in high multiplicity pp collisions at $\sqrt{s} = 7$ TeV, the kinetic freeze-out temperature is around 90 MeV. This indicates that there is a possibility that we may observe BEC in pp collisions at the LHC energies.

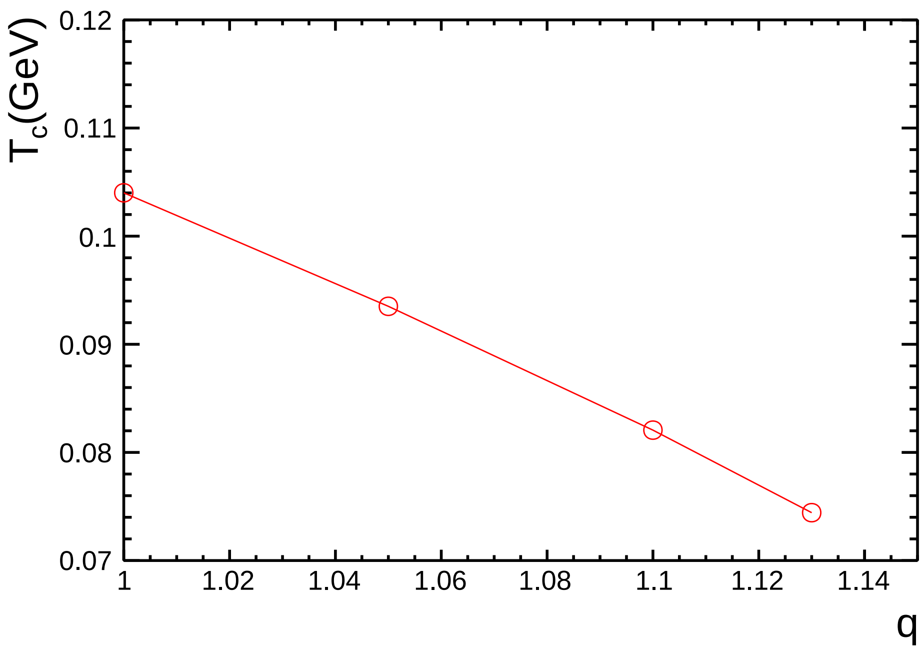

Figure 4.2: (Color online) Critical temperature as a function of non-extensive parameter q.

In Fig.4.2, we have plotted the transition/critical temperatures (T_c) as a function of the non-extensive parameter q. These T_c points are extracted from the Fig.4.1. We observe that for the lower value of q i.e. ($q = 1$) in which the system is at equilibrium, the T_c for BEC is the highest value at around 105 MeV. For higher value of q ($q = 1.13$) in which the system is far away from the equilibrium, the (T_c) for BEC is lower value at around 75 MeV.

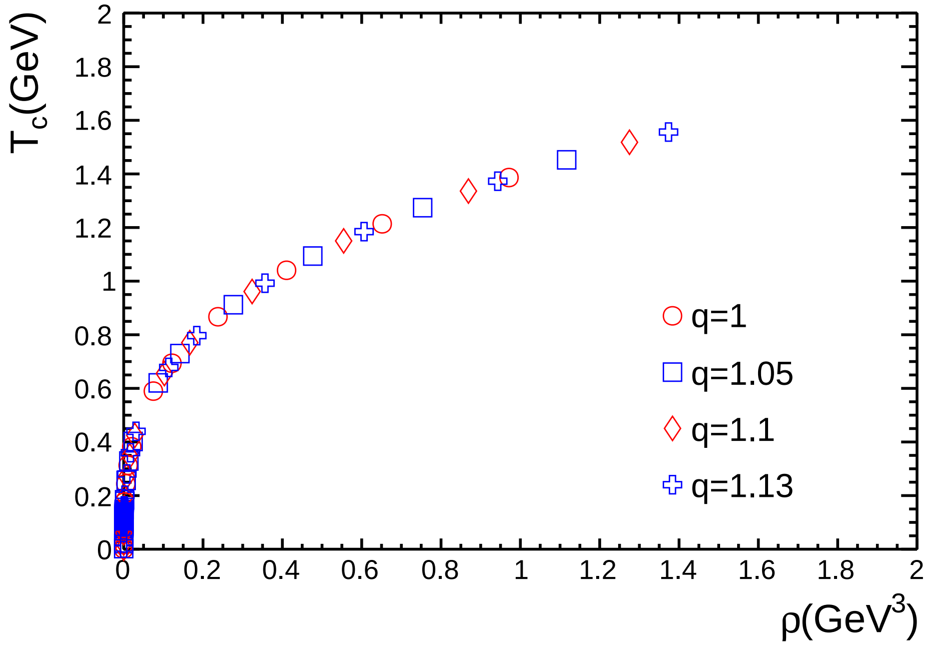

Figure 4.3: (Color online) Critical temperature as a function of number density for pion gas.

The relation between the critical temperature and the number density can be obtained by Eq.(4.7). Fig.4.3 shows the critical temperature (T_c) as a function of number density (ρ). To estimate ρ we have used the Eq.(4.8) for certain T and q values. We see that the critical temperature is only dependent on number density ρ, higher the number density, higher is the critical temperature of the system.

In Fig.4.4, we have plotted the ratios of $N_{\text{condensation}}$ to N_{total} and N_{excited} to N_{total} for pp collisions at $\sqrt{s} = 7$ TeV using the ALICE data as a function of charged particle multiplicity. In this case, the kinetic freeze-out temperatures with corresponding q values are obtained after fitting Tsallis distribution function to its p_T-spectra of charged pions [15]. For the sake of simplicity, we have only considered the chemical freeze-out

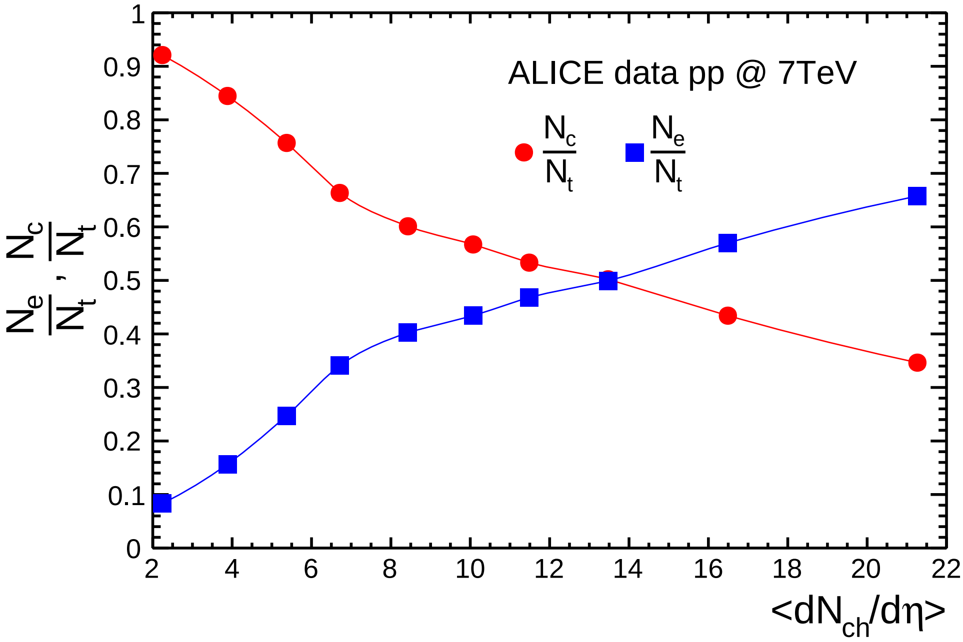

Figure 4.4: (Color online) Ratios of number of particles in the condensate with total number of particles and number of particles in the excited state with total number of particles as a function of charged particle multiplicity for pp collisions at $\sqrt{s} = 7$ TeV at the ALICE.

volume of the system which can vary with the system's different chemical freeze-out radii corresponding to each charged particle multiplicities [16]. We observe that at high charged particle multiplicity which corresponds to higher kinetic freeze-out temperature, about 70% of the particles are in the excited states and about 30% of the particles occupy the lowest quantum state. With the decrease in $\langle dN_{\rm ch}/d\eta\rangle$ we see that the $N_{\rm excited}$ to $N_{\rm total}$ ratio is decreasing while the $N_{\rm condensation}$ to $N_{\rm total}$ ratio is increasing. At about $\langle dN_{\rm ch}/d\eta\rangle = 14$, which corresponds to 87 MeV temperature, we observe a transition. This $\langle dN_{\rm ch}/d\eta\rangle$ can be considered as the critical charged particle multiplicity for pp collisions at $\sqrt{s} = 7$ TeV at the LHC, before which the number of particles in the condensate is higher than the excited states. At the lowest charged particle multiplicity, we observe that the particle multiplicity in the condensate is dominant over the particles at the excited states. This is an interesting finding given that at low charged particle multiplicity the number density, the volume and the temperature of the system are relatively lower as compared to the systems at high charged particle multiplicities.

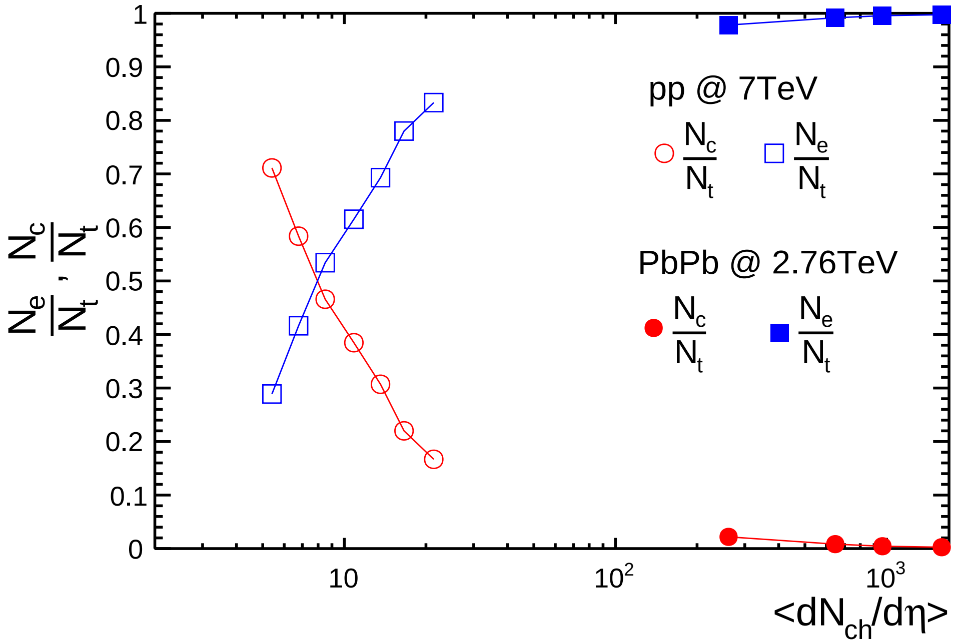

Figure 4.5: (Color online) Ratios of number of particles in the condensate with total number of particles and number of particles in the excited state with total number of particles as a function of charged particle multiplicity for pp collisions at $\sqrt{s}$ = 7 TeV and Pb-Pb collisions at $\sqrt{s_{\rm NN}}$ = 2.76 TeV at the ALICE.

Getting the volume of the system formed in a collision system is not trivial. To get an approximate value, we have used the chemical freeze-out radius estimated from the HBT (Hanbury-Brown-Twiss) radius, and we have added a factor 0.4 of hadronic phase lifetime of the system at certain charged particle multiplicities [17] to get the total approximate radius of the system at kinetic freeze-out. Using this, we have estimated the volume of the systems and later used it in our estimations.

In Fig.4.5, in pp collisions, we observe a smooth transition from the collision species. It shows that at around $\langle dN_{\rm ch}/d\eta\rangle \sim 8$, we may observe BEC. For Pb-Pb collisions at $\sqrt{s_{NN}}$ = 2.76 TeV almost all of the particles are in the excited state and the number of particles in the ground state increases slowly as we move towards peripheral Pb-Pb collision systems. The condensate is more dominant at peripheral collisions than central collisions.

4.4 Summary and Conclusions

The presence of high fraction of condensation in the particle spectra of low multiplicity proton-proton collisions arises the possibility that the BEC-like effect in spectra can also be due to non-equilibrium effects. This is because the local thermalization is less expected in the low multiplicity region. It may be a hint that BEC-like features can be observed due to some other effect like non-equilibrium at low multiplicity which is mimicking the effect of BEC. This can be a consequence of strong correlation in the system, rather than due to attainment of BE equilibrium and consequent condensation. So this result shows that interpretation of BEC in high energy collisions should be done carefully, to confirm that really an equilibrium condensation is achieved according to BE statistics.

We observed that the critical temperature (T_c) of BEC is highly dependent on the thermodynamically consistent non-extensive parameter q. Finally we estimated theoretically that there is a possibility of BEC in the pion gas formed in pp collisions.

Bibliography

[1] Raghunath Sahoo, Relativistic Kinematics, [nucl-ex] (2016).

[2] J. Adams, *et al* [STAR Collaboration], *Nucl.Phys.A* **757**, 102 (2005).

[3] Raghunath Sahoo, Possible Formation of QGP-droplets in Proton-Proton Collisions at the CERN Large Hadron Collider, [nucl-ex], AAPPS Bulletin, Vol. 29, Page. 16 (2019).

[4] F. Karsch, E. Laermann and A. Peikert, Quark Mass and Flavour Dependence of the QCD Phase Transition, *Nucl.Phys.B* **605**, 579 (2001).

[5] O. Penrose, Foundations of Statistical Mechanics: A Deductive Treatment (Pergamon Press, Oxford, 1970).

[6] C. Tsallis, Introduction to Non-extensive Statistical Mechanics (Springer Science, 2009).

[7] R. Hagedorn, Statistical thermodynamics of strong interactions at high energies, *Nuovo Cimento Supplements*, **3**, 147 (1965).

[8] D. Thakur, S. Tripathy, P. Garg, R. Sahoo, J. Cleymans, Indication of a Differential Freeze-out in Proton-Proton and Heavy-Ion Collisions at the RHIC and the LHC energies, *Adv.High Energy Phys.* 2016 4149352 (2016).

[9] J. Cleymans and D. Worku, The Tsallis distribution in proton-proton collisions at $\sqrt{s} = 0.9$ TeV at the LHC, *J. Phys. G: Nucl Part. Phys.* **39** 025006 (2012).

[10] M. D. Azmi *et al*, Energy density at kinetic freeze-out in Pb-Pb collisions at the LHC using the Tsallis distribution, *J. Phys. G: Nucl. Part. Phys.* **47** 045001 (2020).

[11] A. Guha and P. K. Das, An Extensive Study of Bose-Einstein Condensation in Liquid Helium using Tsallis Statistics, *Physica A* **497**, 272 (2018).

[12] V. Begun and M. Gorenstein, Bose-Einstein Condensation of Pions, PoS CPOD07:047 (2007).

[13] V. Begun and W. Florkowski, Bose-Einstein condensation of pions in heavy-ion collisions at the CERN Large Hadron Collider (LHC) energies, *Phys. Rev. C* **91**, 054909 (2015).

[14] V. Begun, High temperature Bose-Einstein condensation, *EPJ Web Conf.* **126** 03002 (2016).

[15] A. Khuntia, H. Sharma, S. K. Tiwari, R. Sahoo, J. Cleymans, Radial flow and differential freeze-out in proton-proton collisions at $\sqrt{s} = 7$ TeV at the LHC, *Eur.Phys.J.A* **55** 3 (2019).

[16] Natasha Sharma *et al*, A Comparison of p-p, p-Pb, Pb-Pb Collisions in the Thermal Model: Multiplicity Dependence of Thermal Parameters, *Phys.Rev.C* **99** 044914 (2019).

[17] D. Sahu, S. Tripathy, G. S. Pradhan, R. Sahoo, Role of event multiplicity on hadronic phase lifetime and QCD phase boundary in ultra-relativistic collisions at energies available at the BNL Relativistic Heavy Ion Collider and the CERN Large Hadron Collider, *Phys. Rev. C* **101**, 014902 (2020).